Angewandte
Eine Zeitschrift der Gesellschaft Deutscher Chemiker
Chemie

Supporting Information

Site-Specific Oxidation State Assignments of the Irons in the [4Fe:4S]$^{2+/1+/0}$ States of the Nitrogenase Fe-Protein

Belinda B. Wenke[+], *Thomas Spatzal*[+], *and Douglas C. Rees**

anie_201813966_sm_miscellaneous_information.pdf

Supporting Information

Table of Contents

Experimental Section

Protein isolation: Following previously described protocols[1–3], *Azotobacter vinelandii* cells were grown aerobically and nitrogenase expression was induced by ammonia depletion. Nitrogenase proteins from *A. vinelandii* were purified anaerobically using Schlenk line techniques and assessed for activity using acetylene reduction assays. The specific activity for acetylene reduction averaged 2010 ± 100 nmol of ethylene min^{-1} mg^{-1} for Mo-Fe protein and 1970 ± 100 nmol of ethylene min^{-1} mg^{-1} for Fe-protein. Nitrogenase protein solutions were buffered in 50 mM Tris/HCl pH 7.5, 200 mM NaCl, 5 mM sodium dithionite. Ti(III) citrate was prepared from a 1.5% solution of Ti(III) chloride in 0.2 M sodium citrate, neutralized to pH 7.0 by titrating in sodium carbonate.

Crystallization: All crystals were obtained by vapor-diffusion sitting-drop techniques in 95% Ar, 5% H_2 atmosphere, 25°C. *A. vinelandii* Fe-protein was used at concentrations between 20-40 mg/mL.

ADP-bound crystal formation: The dithionite-reduced, ADP-bound crystals were identified from a condition containing Fe-protein and MoFe-protein at a 4:1 molar ratio, with 1 mM $AlCl_3$, 10 mM NaF, 5 mM ATP and 10 mM $MgCl_2$ to form an aluminum fluoride stabilized protein complex. A 100 kDa molecular weight cut-off concentration unit (EMD Millipore) was used to separate free Fe-protein, but Fe-protein was retained in the mixture used for crystal trials. Evidently, a population of Fe-protein hydrolyzed MgATP, resulting in crystallized Fe-protein-MgADP. The crystals were obtained in 40% PEG 400, 0.17 mM Cymal 7, 0.1 M HEPES pH 7.5, 5 mM dithionite. Oxidized structures were obtained by first growing crystals in the dithionite-reduced, MgADP condition, and soaking the crystals in 5 mM indigocarmine (IDS) for 1 – 5 min. The progress of the crystal soaks was apparent by the change in color of the crystals from ~brown to ~green over time. Crystals were cryo-protected with 2-methyl-2, 4-pentanediol (MPD). Ti(III) citrate-reduced protein was screened for an ADP-bound form, but the trials did not yield crystals.

Nucleotide-free crystal formation: Crystals of the dithionite-reduced, nucleotide free state were grown in a solution of 40% PEG 1000, 0.2 M NaCl, 0.1 M MES/OH pH 6.5, 10%

2,2,2-trifluoroethanol, 5 mM dithionite, and cryo-protected with 2-methyl-2, 4-pentanediol (MPD). All-ferrous crystal structures were grown in conditions of 37% PEG 3350, 0.05 M NaCl, 0.1 M Bis/Tris pH 5.5, 5 mM Ti(III) citrate. Crystals of the IDS-oxidized nucleotide-free form were prepared from the dithionite-reduced nucleotide free crystals, but yielded poor diffraction.

Structure determination: Crystallographic data were collected at the Stanford Synchrotron Radiation Lightsource at beamline 12-2, using 0.5° steps over 360°. The high-resolution Fe protein structure was obtained in the orthorhombic space group $P22_12_1$ with cell constants of a = 45.7 Å, b= 74.6 Å, c= 75.2 Å (for additional crystallographic statistics, see Table S2). The crystals grew in space group $P22_12_1$, with one subunit per asymmetric unit (previous Fe-protein crystals have exclusively contained the full dimer in the asymmetric unit). Datasets were collected at multiple wavelengths (see Table S3) across the iron K-edge (7121 eV). Spatially resolved anomalous dispersion refinement (SpReAD) analysis was performed as previously reported by refining Δf'' values against the anomalous differences for individual structure factors[4,5], with phases calculated from the structure refined against the high-resolution dataset collected at 12,000 eV. The data were integrated with XDS[6] and merged with SCALA[7]. The high-resolution structures collected at 12,000 eV were phased with PHASER by molecular replacement using one monomer of the previously determined Fe protein structure (1G5P)[8], with the [4Fe:4S] cluster omitted. For the refinement, the standard ligands SF4 and FES were used from the CCP4 library (FES Fe-Fe bond distance: 3.06 Å, Fe-S bond lengths: 2.20 Å. SF4 Fe-Fe bond lengths: 3.10 Å, Fe-S bond distance: 2.19 Å). We note that the Fe-Fe distances in these standard groups are significantly longer than observed in actual FeS clusters (~2.70 Å). The holo structures were refined with Refmac5 in the CCP4 suite, and provided the phases for the high-energy datasets[9]. Model building was performed in Coot[10]. For an overlay of all SpReAD profiles, see Figure S3. The nucleotide observed was assigned as MgADP based on the coordination sphere of the Mg^{2+} ion; we observed a hexacoordinate ion adjacent to the ADP molecule, liganded to four waters, Ser16 and a phosphate from ADP. The Mg^{2+}-ligand distances are ~2.1 Å, consistent with $Mg^{2+}(H_2O)$ complexes[11]. An AlF_4^- molecule would have predicted ~1.7 Å bond lengths for Al-F[12],

with a square planar geometry and a binding site distinct from the Mg^{2+} ion, as observed in the 1M34 complex structure[13].

The coordinates and structure factors have been deposited in the RCSB Protein Data Bank entries: 6N4J (Ti(III)-citrate reduced, nucleotide free form), 6N4K (DT-reduced, nucleotide free form), 6N4L (DT-reduced, ADP-bound form), 6N4M (IDS-oxidized, ADP-bound form).

Electron paramagnetic resonance: EPR experiments were performed on an X-band Bruker EMX CW-EPR spectrometer with an ESR 900 liquid helium/nitrogen flow-through cryostat (Oxford Instruments) at powers ranging from 2 mW to 10 mW at 10 K. The modulation amplitude was 3 G and the modulation frequency 100 kHz, with a 40 ms time constant and 167.7 s sweep time. In the solution-state sample, the protein concentration was 20 mg/mL (0.31 mM) in 18.25% PEG 1000, 0.1 M sodium chloride, 0.05 M MES/OH pH 6.5 and 10 mM sodium dithionite. The crystal slurry sample was prepared by growing *A. vinelandii* Fe-protein crystals in 2 µL sitting drops. 115 clear drops with crystals were pooled in reservoir buffer (36.5% PEG 1000, 0.2 M sodium chloride, 0.1 M MES/OH pH 6.5, 10 mM sodium dithionite) and crystals were broken using a cryo-loop. Samples were frozen in liquid nitrogen in 4 mm thin-wall quartz tubes (Wilmad-Lab Glass). Simulations were performed using GeeStrain5[14]. Simulation parameters: g = (1.85, 1.927, 2.00), σg = (0.023, 0.010, 0.045).

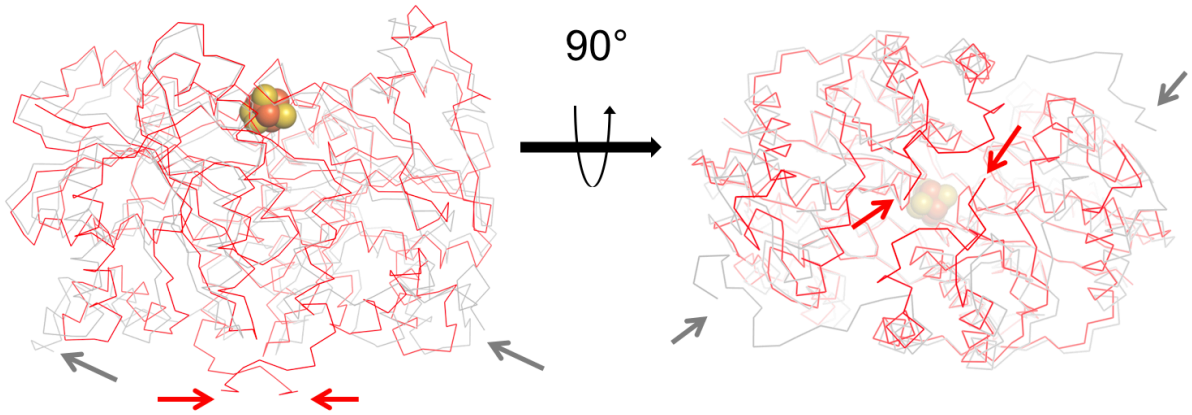

Figure S1. Overlay of the previously reported Fe-protein structure (1G5P, gray) and the 1.13 Å-resolution, Mg-ADP-bound structure determined in this work (red). C-termini are indicated with gray and red arrows, respectively.

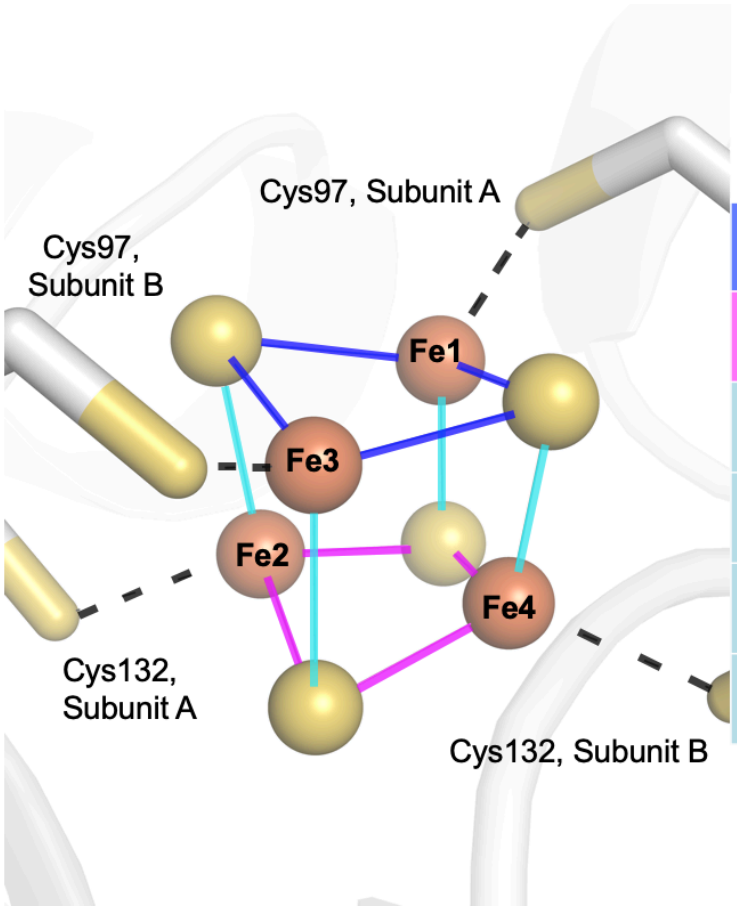

	Cluster charge			
D (Å)	0	1+	1+ (ADP)	2+ (ADP)
Fe1-Fe3	2.86	2.68	2.76	2.73
Fe2-Fe4	2.82	2.64	2.78	2.77
Fe1-Fe2	2.81	2.64	2.70	2.69
Fe1-Fe4	2.84	2.67	2.63	2.61
Fe2-Fe3	2.85	2.70	2.63	2.61
Fe3-Fe4	2.84	2.64	2.70	2.69
AVG	2.84	2.66	2.70	2.68
STDEV	0.02	0.03	0.06	0.06

Figure S2. Fe-S distances in the cluster across oxidation states. Fe1-Fe4 are coordinated by Sγ of Cys A97, Cys A132, Cys B97 and Cys B132, respectively.

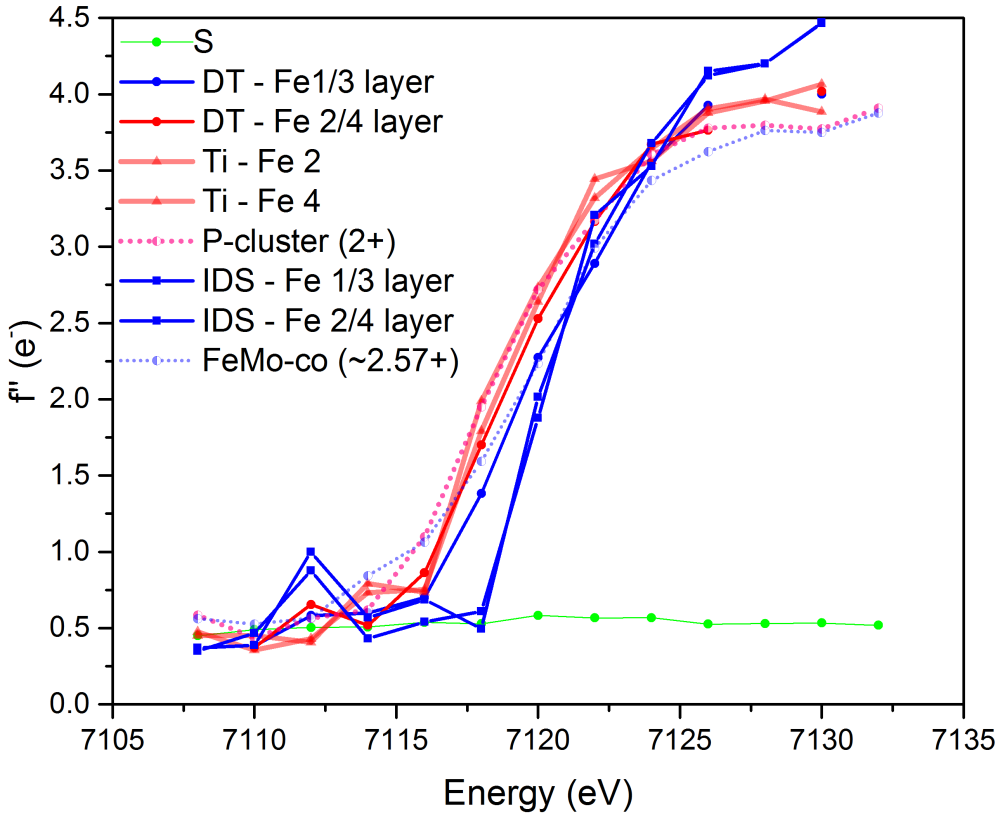

Figure S3. SpReAD profiles for $[4Fe:4S]^{2+}$, $^{1+}$ and ^{0} states with average profiles for the P-cluster and FeMo-cofactor[5].

	0+	1+	1+ (MgADP)	2+ (MgADP)
1G5P	0.627	0.666	0.745	0.687
1G1M	0.322	0.570	0.727	0.648
1FP6	0.693	0.731	0.576	0.449

Table S1. Cα RMSD (Å) between Fe-protein in different oxidation and nucleotide states reported in here and previously, including the nucleotide free forms of the $[4Fe:4S]^{1+}$ (PDB entry 1G5P) and $[4Fe:4S]^{0}$ (PDB entry 1G1M) oxidation states, and the ADP-bound form of the $[4Fe:4S]^{1+}$ state (PDB entry 1FP6) using Chimera[15].

	0+ (-MgADP)	**0+ SpReAD**	**1+ (-MgADP)**	**1+ SpReAD**	**1+ (+MgADP)**	**1+ SpReAD**	**2+ (+MgADP)**	**2+ SpReAD**
Wavelength (eV)	12000	7100-7130	12000	7100-7130	14000	7080-8010	12000	7080-8010
Resolution range (Å)	44.68-1.95 (2.06-1.95)	[(2.27-2.05)]	39.29-1.76 (1.82-1.76)	[(2.06-2.05)]	39.01-1.13 (1.15-1.13)	[(2.0-1.80)]	39.03-1.58 (1.67-1.58)	[(2.11-1.92)]
Space group	$P2_1$		C2		$P22_12_1$		$P22_12_1$	
Unit cell parameters	57.25 Å		103.81 Å		45.59 Å		45.81 Å	
	93.05 Å		45.30 Å		74.63 Å		74.58 Å	
	60.77 Å		109.05 Å		75.40 Å		75.02 Å	
	90° 98.5° 90°		90° 96.6° 90°		90° 90° 90°		90° 90° 90°	
Mean I/σ	11.2 (2.2)		8.1 (1.7)		17.6 (3.0)		31.2 (3.7)	
CC(1/2)	0.999 (0.930)		0.998 (0.847)		0.999 (0.915)		1.000 (0.897)	
Completeness (%)	90.04 (92.4)	[96.6- 93.5 (89.8-79.5)]	96.1 (55.7)	[92.8-92.2 (76.1- 75.9)]	100 (99.9)	[99.1- 85.4 (90.0-90.3)]	98.9 (97.8)	[95.0-94.4 (71.3-68.9)]
R_{pim} (all I+ & I-)	0.026 (0.211)	[0.023-0.021 (0.384-0.217)]	0.019 (0.278)	[0.040-0.039 (0.187-0.143])	0.020 (0.239)	[0.020-0.018 (0.357-0.107)]	0.016 (0.250)	[0.017-0.016 (0.343-0.235)]
Total unique reflections	41566 (6160)	[31666-31542 (4527-2373)]	51971 (1562)	[60171-59309 (7230-7046)]	96897 (13986)	[21154-17961 (1165-1172]	35382 (5009)	[23855-16472 (8519-8092)]
Bond length RMSD (Å)	0.021		0.017		0.029		0.023	
Bond angles RMSD (°)	2.430		2.232		2.658		2.158	
R_{factor}	0.2108		0.1684		0.1364		0.1763	
R_{free}	0.2471		0.2197		0.1539		0.1908	

Table S2. Crystallographic data table for Fe-protein in 0+, 1+, and 2+ oxidation states. Statistics in the high-resolution shell are indicated with round brackets. The data used in the SpReAD analysis is given as a range of values, denoted with square brackets.

Energy (eV)	P-cluster (2+)	FeMo-co (2.57+)	S	Fe 1 (TiCi)	Fe 2 (TiCi)	Fe 3 (TiCi)	Fe 4 (TiCi)	Fe 1 (DT)	Fe 2 (DT)	Fe 3 (DT)	Fe 4 (DT)
7108	0.584	0.515	0.450	0.364	0.451	0.396	0.475	0.372	0.420	0.358	0.411
7110	0.437	0.447	0.490	0.445	0.451	0.333	0.356	0.387	0.463	0.389	0.348
7112	0.564	0.517	0.504	0.260	0.407	0.309	0.430	0.455	0.541	0.579	0.511
7114	0.619	0.818	0.507	0.796	0.792	0.733	0.733	0.763	0.914	0.829	0.845
7116	1.099	1.098	0.538	0.765	0.735	0.632	0.753	0.707	0.675	0.65	0.661
7118	1.949	1.589	0.529	1.948	1.988	1.796	1.792	1.409	1.801	1.318	1.733
7120	2.720	2.138	0.583	2.672	2.733	2.593	2.639	2.468	2.756	2.321	2.645
7122	3.174	2.733	0.567	3.323	3.320	3.237	3.445	2.983	3.266	2.970	3.220
7124	3.605	3.167	0.568	3.628	3.644	3.549	3.563	3.514	3.698	3.483	3.635
7126	3.778	3.460	0.525	3.960	3.906	3.774	3.877	3.779	3.926	3.624	3.683
7128	3.797	3.638	0.529	3.938	3.967	3.916	3.957	3.648	3.917	3.878	3.766
7133	3.773	3.717	0.534	3.963	3.886	3.990	4.065	3.766	3.803	3.652	3.735

Energy (eV)	P-cluster (2+)	FeMo-cofactor (2.57+)	S	Fe 1,3 (DT +ADP)	Fe 2,4 (DT+ADP)	Fe 1,3 (IDS + ADP)	Fe 2,4 (IDS + ADP)
7108	0.584	0.515	0.450	--	--	0.370	0.350
7110	0.437	0.447	0.490	0.382	0.373	0.387	0.467
7112	0.564	0.517	0.504	0.582	0.655	0.999	0.878
7114	0.619	0.818	0.507	0.600	0.518	0.568	0.430
7116	1.099	1.098	0.538	0.700	0.864	0.686	0.541
7118	1.949	1.589	0.529	1.382	1.700	0.496	0.609
7120	2.720	2.138	0.583	2.273	2.527	2.016	1.876
7122	3.174	2.733	0.567	2.891	3.164	3.018	3.206
7124	3.605	3.167	0.568	3.555	3.673	3.679	3.529
7126	3.778	3.460	0.525	3.927	3.764	4.122	4.152
7128	3.797	3.638	0.529	--	--	4.200	4.200
7133	3.773	3.717	0.534	4.000	4.018	4.466	4.471

Table S3. f'' values as a function of energy for observed oxidation states, nucleotide free (top) and ADP-bound (bottom).

References

[1] D. Wolle, C. Kim, D. Dean, J. B. Howard, *J. Biol. Chem.* **1992**, *267*, 3667–3673.
[2] T. Spatzal, M. Aksoyoglu, L. Zhang, S. L. Andrade, E. Schleicher, S. Weber, D. C. Rees, O. Einsle, *Science* **2011**, *334*, 940–940.
[3] T. Spatzal, K. A. Perez, O. Einsle, J. B. Howard, D. C. Rees, *Science* **2014**, *345*, 1620–1623.
[4] O. Einsle, S. L. Andrade, H. Dobbek, J. Meyer, D. C. Rees, *J. Am. Chem. Soc.* **2007**, *129*, 2210–2211.
[5] T. Spatzal, J. Schlesier, E.-M. Burger, D. Sippel, L. Zhang, S. L. Andrade, D. C. Rees, O. Einsle, *Nat. Commun.* **2016**, *7*, 10902.
[6] W. Kabsch, *Acta Crystallogr. Sect. D* **2010**, *66*, 133–144.
[7] P. Evans, *Acta Crystallogr. D Biol. Crystallogr.* **2006**, *62*, 72–82.
[8] P. Strop, P. M. Takahara, H.-J. Chiu, H. C. Angove, B. K. Burgess, D. C. Rees, *Biochemistry* **2001**, *40*, 651–656.
[9] M. D. Winn, G. N. Murshudov, M. Z. Papiz, in *Methods Enzymol.*, Elsevier, **2003**, pp. 300–321.
[10] P. Emsley, K. Cowtan, *Acta Crystallogr. D Biol. Crystallogr.* **2004**, *60*, 2126–2132.
[11] D. Rutkowska-Zbik, M. Witko, L. Fiedor, *J. Mol. Model.* **2013**, *19*, 4661–4667.
[12] Y.-W. Xu, S. Moréra, J. Janin, J. Cherfils, *Proc. Natl. Acad. Sci.* **1997**, *94*, 3579–3583.
[13] B. Schmid, O. Einsle, H.-J. Chiu, A. Willing, M. Yoshida, J. B. Howard, D. C. Rees, *Biochemistry* **2002**, *41*, 15557–15565.
[14] W. R. Hagen, *Biomolecular EPR Spectroscopy*, CRC Press, **2008**.
[15] E. F. Pettersen, T. D. Goddard, C. C. Huang, G. S. Couch, D. M. Greenblatt, E. C. Meng, T. E. Ferrin, *J. Comput. Chem.* **2004**, *25*, 1605–1612.